Electrically-Active Convection in Tropical Easterly Waves and Implications for Tropical Cyclogenesis in the Atlantic and East Pacific

K. Leppert II, Dept. Atmospheric Science, University of Alabama in Huntsville
W. Petersen, NASA GSFC/WFF (walt.petersen@nasa.gov)
D. Cecil, Earth Systems Sciences Center, University of Alabama in Huntsville

One possible key to improving tropical cyclone initiation forecasting is to understand how a given tropical wave disturbances acts to organize areas of deep convection and precipitation that form the "seeds" of incipient tropical storms and/or hurricanes. Because on average only one in ten tropical waves tend to develop tropical cyclones, it is beneficial to be able to recognize clues that suggest eventual intensification of any given wave. Related questions would be: Can satellite remote sensing tools be used to identify incipient cyclone "seeds" of intensification within a given tropical wave? More specifically, can the observed strength and evolution of deep convective storms and precipitation typically observed in tropical disturbances be used as a metric for indications of future tropical cyclone development?

To answer the aforementioned questions, in this study we investigate the evolution of individual convective storm structures within tropical easterly waves across the Atlantic and Eastern Pacific Ocean Basins. We examine diagnostics of convective storm intensity (infrared cloud top temperatures, lightning, and microwave brightness temperatures) as a function of the surrounding environment (e.g., large scale mass and moisture convergence profiles in the disturbances) as a means to assess the mechanisms by which convective storms might influence cyclone development and the potential role/use of convective storm intensity observations for predicting tropical cyclogenesis. We use data from the Tropical Rainfall Measurement Mission (TRMM) satellite Microwave Imager (TMI), Precipitation Radar (PR), and Lightning Imaging Sensor (LIS) as well as infrared (IR) brightness temperature data from the NASA global-merged IR brightness temperature dataset to evaluate convective storm intensities within given easterly waves across the Atlantic and Pacific regions of study and how those intensity diagnostics differ between tropical easterly waves that do or do not spawn tropical cyclones

The study results suggest that convective storm intensity diagnostics that best distinguish developing from non-developing cyclone waves vary as a function of where a given wave actually spawns a tropical cyclone. For waves that develop cyclones in the Atlantic basin, coverage by IR brightness temperatures less than 240 K and 210 K seems to provide the best distinction between developing and non-developing waves. Over the East Pacific several variables seem to provide a significant distinction between cyclone-developing and non-developing waves. These variables include the same IR temperature coverage thresholds as observed in the Atlantic Basin, in addition to lightning flash rate, and low-level (<4.5 km) PR reflectivity which are all increased in the convection of easterly waves that develop cyclones. The results of this study are consistent with previously hypothesized feedbacks between wave convective structures and tropical cyclogenesis, and also reasonably suggest that satellite remote sensing diagnostics that discern the intensity of storm clusters within tropical disturbances may provide some guidance for distinguishing waves that are or are not likely to develop tropical cyclones.

Monthly Weather Review

Electrically-Active Convection in Tropical Easterly Waves and Implications for Tropical Cyclogenesis in the Atlantic and East Pacific

--Manuscript Draft--

Manuscript Number:	
Full Title:	Electrically-Active Convection in Tropical Easterly Waves and Implications for Tropical Cyclogenesis in the Atlantic and East Pacific
Article Type:	Article
Corresponding Author:	Kenneth David Leppert II University of Alabama in Huntsville Huntsville, AL UNITED STATES
Corresponding Author's Institution:	University of Alabama in Huntsville
First Author:	Kenneth David Leppert II
Order of Authors:	Kenneth David Leppert II
	Walter Petersen
	Daniel Cecil
Abstract:	In this study, we investigate the characteristics of tropical easterly wave convection and the possible implications of convective structure on tropical cyclogenesis and intensification over the Atlantic Ocean and East Pacific using data from the Tropical Rainfall Measurement Mission Microwave Imager, Precipitation Radar (PR), and Lightning Imaging Sensor as well as infrared (IR) brightness temperature data from the NASA global-merged IR brightness temperature dataset. Easterly waves were partitioned into northerly, southerly, trough, and ridge phases based on the 700-hPa meridional wind from the NCEP-NCAR reanalysis dataset. Waves were subsequently divided according to whether they did or did not develop tropical cyclones (i.e., developing and nondeveloping, respectively), and developing waves were further subdivided according to development location. Finally, composites as a function of wave phase and category were created using the various datasets. Results suggest that the convective characteristics that best distinguish developing from nondeveloping waves vary according to where developing waves spawn tropical cyclones. For waves that developed a cyclone in the Atlantic basin, coverage by IR brightness temperatures ≤240 K and ≤210 K provide the best distinction between developing and nondeveloping waves. In contrast, several variables provide a significant distinction between nondeveloping waves and waves that develop cyclones over the East Pacific as these waves near their genesis location including IR threshold coverage, lightning flash rates, and low-level (<4.5 km) PR reflectivity. Results of this study may be used to help develop thresholds to better distinguish developing from nondeveloping waves and serve as another aid for tropical cyclogenesis forecasting.
Suggested Reviewers:	

Electrically-Active Convection in Tropical Easterly Waves and Implications for Tropical Cyclogenesis in the Atlantic and East Pacific

Kenneth D. Leppert II[*]

Walter A. Petersen[+]

and

Daniel J. Cecil[*]

[*]University of Alabama Huntsville, Huntsville, Alabama

[+]NASA GSFC/Wallops Flight Facility Code 610.W, Wallops Island, Virginia

SUBMITTED TO *MONTHLY WEATHER REVIEW* 15 June 2012

*Corresponding author address: Kenneth Leppert II, NSSTC, 320 Sparkman Dr Rm 4074, Huntsville, AL 35805

E-mail: leppert@nsstc.uah.edu

ABSTRACT

In this study, we investigate the characteristics of tropical easterly wave convection and the possible implications of convective structure on tropical cyclogenesis and intensification over the Atlantic Ocean and East Pacific using data from the Tropical Rainfall Measurement Mission Microwave Imager, Precipitation Radar (PR), and Lightning Imaging Sensor as well as infrared (IR) brightness temperature data from the NASA global-merged IR brightness temperature dataset.

Easterly waves were partitioned into northerly, southerly, trough, and ridge phases based on the 700-hPa meridional wind from the NCEP-NCAR reanalysis dataset. Waves were subsequently divided according to whether they did or did not develop tropical cyclones (i.e., developing and nondeveloping, respectively), and developing waves were further subdivided according to development location. Finally, composites as a function of wave phase and category were created using the various datasets.

Results suggest that the convective characteristics that best distinguish developing from nondeveloping waves vary according to where developing waves spawn tropical cyclones. For waves that developed a cyclone in the Atlantic basin, coverage by IR brightness temperatures $\leq$240 K and $\leq$210 K provide the best distinction between developing and nondeveloping waves. In contrast, several variables provide a significant distinction between nondeveloping waves and waves that develop cyclones over the East Pacific as these waves near their genesis location including IR threshold coverage, lightning flash rates, and low-level (<4.5 km) PR reflectivity. Results of this study may be used to help develop thresholds to better distinguish developing from nondeveloping waves and serve as another aid for tropical cyclogenesis forecasting.

1. Introduction

African easterly waves (AEWs) form in the tropical easterlies over east-central Africa (e.g., Burpee 1972; Norquist et al. 1977; Reed et al. 1977; Berry and Thorncroft 2005; Thorncroft et al. 2008) and often form the necessary precursor low-level disturbance for tropical cyclogenesis (Kurihara and Tuleya 1981). These waves are important for tropical cyclogenesis not only in the Atlantic (e.g., Landsea 1993), but also in the East Pacific (e.g., Avila 1991; Avila and Pasch 1992; Molinari and Vollaro 2000; note, however, that not all easterly waves found over the East Pacific originate over Africa; e.g., Serra et al. 2008, 2010).

One outstanding question is why some waves develop tropical cyclones while others do not. Many factors that play a role in determining whether a wave develops involve the environment through which an easterly wave propagates. For example, a wave may be more likely to develop a tropical cyclone if it propagates through a region of weak vertical wind shear, SSTs >27°C, below-average sea-level pressure, above-normal low-level relative vorticity, and/or above-average precipitable water (all conditions favorable for tropical cyclogenesis; e.g., Gray 1968; Landsea et al. 1998; Bracken and Bosart 2000).

Hopsch et al. (2010) suggest that the structure of AEWs near the West African coast may be another important influence for determining the likelihood of cyclone development. In that study, developing waves were associated with higher values of relative humidity as well as stronger mid- and low-level circulations compared to nondeveloping waves (NDWs). In addition, it was found that developing waves tend to undergo a transformation from a cold-core structure over the African continent to a warm-core structure at the coast and over the ocean, consistent with cyclogenesis, while NDWs showed no such transformation. Results of Hopsch et

al. (2010) also indicated that differences in the structure of developing waves and NDWs at the coast could influence the likelihood of development out to 60°W over the Atlantic Ocean.

Easterly waves are often associated with convection at some point in their lifetime (e.g., Burpee 1974; Thompson et al. 1979; Duvel 1990; Petersen et al. 2003; Petersen and Boccippio 2004; Leppert and Petersen 2010; hereafter LP10), and differences in the nature of this convection between different waves may be another determinant for why some waves develop while others do not. Via thermodynamic and dynamic feedbacks between the smaller convective scale and larger synoptic scale, more intense and/or widespread convection associated with developing waves could help to produce conditions in the wave more favorable for development.

One possible effect of convection on the larger scale favorable for tropical cyclogenesis is an increase in mid- to low-level vorticity. Ritchie and Holland (1997) showed how many midlevel, convective-scale vortices created by convection can interact and merge, resulting in one larger, cyclonic circulation (i.e., mesoscale convective vortex), helping to increase midlevel vorticity on a larger scale. Hendricks et al. (2004) and Montgomery et al. (2006) used numerical model simulations to describe a similar process near the surface whereby convection can help to increase low-level vorticity and aid cyclogenesis. In particular, intense convective towers (i.e., vortical hot towers) were found to acquire large values of vertical vorticity via the tilting and stretching of preexisting vorticity by convective updrafts. Montgomery et al. (2006) suggest that a population of many growing, merging, and decaying towers acts as a quasi-steady diabatic heating rate which feeds back to the large-scale circulation. In order for the circulation to remain in thermal wind balance a secondary radial circulation develops with inflow near the surface. This near-surface inflow encourages vortex merger, the concentration of low-level vorticity, and the intensification of the cyclone (Hendricks et al. 2004; Montgomery et al. 2006). Several

observation-based studies have also provided evidence for the importance of hot towers for increasing low-level vorticity and aiding tropical cyclogenesis (e.g., Reasor et al. 2005; Sippel et al. 2006; Houze et al. 2009).

Another potential contribution of persistent, widespread convection to the genesis process is the moistening of mid and upper levels via transport of moisture from the surface. In particular, Dunkerton et al. (2009) emphasizes the importance for tropical cyclogenesis of the containment and accumulation of moisture transported by convection within a Lagrangian re-circulation region of the trough phase of an easterly wave. This moisture transport and/or accumulation inhibits the development of evaporatively-cooled downdrafts and associated transport of low equivalent potential temperatures to the surface, which is thought to inhibit tropical cyclogenesis (Rotunno and Emanuel 1987). Nolan (2007) also showed the importance of mid- and upper-level moistening for tropical cyclogenesis.

Because enhanced convection could potentially enhance the development of an easterly wave circulation and structure more favorable for tropical cyclogenesis, it is not surprising that previous studies have found developing waves to be associated with more intense and/or widespread convection compared to NDWs. For example, Hopsch et al. (2010) used IR brightness temperatures to determine that developing waves are, in fact, associated with more widespread/intense convection. Chronis et al. (2007) used lightning frequency to infer the intensity of convection and found that tropical cyclogenesis in the East Atlantic may be related to enhanced electrical activity (i.e., more intense convection) over that region. In this case, lightning represents a proxy for deep convective updrafts and robust mixed-phase microphysical processes, previously demonstrated to be a prerequisite for the development of strong in-cloud electric fields and associated lightning (e.g., Takahashi 1978; Rutledge et al. 1992; Williams et

al. 1992; Zipser 1994; Saunders and Peck 1998; Deierling and Petersen 2008). In addition, Price et al. (2007) showed that enhanced lightning over East Africa may also be associated with cyclogenesis over the East Atlantic. Leary and Ritchie (2009) examined cloud clusters instead of waves in the East Pacific and found that developing cloud clusters were associated with significantly more lightning than nondeveloping clusters. LP10 examined IR brightness temperatures as well as lightning associated with AEWs over several longitude bands stretching from East Africa (30°E) to the central Atlantic (50°W). They found that over each longitude band developing waves were associated with a greater coverage of more intense, electrically-active convection compared to NDWs.

This study expands on previous studies by not only examining lightning and/or IR brightness temperatures for clues about convection related to tropical cyclogenesis but also examining microwave brightness temperatures from the Tropical Rainfall Measurement Mission (TRMM) Microwave Imager (TMI) and radar reflectivity data from the TRMM Precipitation Radar (PR). In particular, the purpose of this study is twofold: 1.) Determine which observations/characteristics of convection provide the best distinction between developing waves and NDWs. 2.) Determine whether the characteristics that provide the best distinction vary for waves that develop tropical cyclones over different regions. This paper composites all easterly wave observations over fixed regions (i.e., Eulerian framework), while a companion study (Leppert and Cecil 2012) examines composites in a wave-following, Lagrangian sense. The Eulerian methodology and the associated results from this paper could potentially be used to help distinguish developing waves from NDWs for forecasting applications. In contrast, the Lagrangian methodology used in Leppert and Cecil (2012) requires a priori information describing when and where a wave developed a tropical cyclone, limiting its direct application to

the forecasting process. But, the Lagrangian framework can provide information on the evolution of waves in the days leading up to cyclogenesis (i.e., a greater understanding of the genesis process) that cannot be obtained from the Eulerian approach.

2. Data/Methodology

Following the methodology of LP10, we analyzed easterly waves by partitioning the waves into phases (ridge, northerly, trough, and southerly phases) based on NCEP-NCAR reanalysis (Kalnay et al. 1996) 700-hPa meridional wind data (note that the reanalysis has a spatial [temporal] resolution of 2.5° [six hours; averaged to one day for this study]). Specifically, the various wave phases were identified by first calculating a daily average meridional wind value between 5°–20°N and then calculating a meridional wind anomaly (relative to the mean at each longitude) for each day and longitude. Next, a 3–7 day bandpass filter was applied to the anomalies in order to isolate the period of the easterly waves. The filtered anomalies were subsequently normalized by the standard deviation valid at each longitude, and the ±0.75 standard deviation threshold was used to identify the individual wave phases. In particular, normalized anomalies greater (less) than 0.75 (-0.75) were classified as the southerly (northerly) phase. For a given day, values between northerly (southerly) and southerly (northerly) phases were identified as trough (ridge) phases. Finally, to classify many of those data points unable to be classified using meridional wind data alone, 700-hPa vorticity was calculated using reanalysis zonal and meridional wind components and processed exactly as the meridional wind data.

The analysis domain over which the wave phases were identified for this study was larger than that used in LP10 and stretched from 130°W to 20°E and from 5°N to 20°N, outlined in Fig.

1. To examine the evolution of convection and cold cloudiness associated with the waves as they propagated through our analysis domain, the full analysis domain was divided into five longitude bands, also shown in Fig. 1. These bands stretched from 130°W to 95°W over the East Pacific (EPC), from 95°W to 70°W over the Western Caribbean and far eastern Pacific region (CAR; this band includes the Central American land mass as well as the northern part of South America), from 70°W to 40°W over the West Atlantic (WAT), from 40°W to 15°W over the East Atlantic (EAT; the eastern boundary of this band lies approximately along the West African coast), and from 15°W to 20°E over Africa (AFR). The waves were analyzed for the months of June–November for the 10-year span of 2001–2010. These are the months in which easterly waves are the most pronounced (e.g., Carlson 1969; Gu et al. 2004) and when tropical cyclones often develop in the Atlantic and East Pacific regions (National Hurricane Center [NHC] storm reports; NHC 2011).

After the various wave phases were identified, the wave troughs were divided into developing (i.e., waves that developed tropical cyclones that attained at least tropical storm strength) and NDWs (i.e., waves that never developed a tropical cyclone; see Table 1 for acronyms and definitions of each wave category used in this study) via information provided by NHC (2011). In addition, developing waves were divided based on the longitude band over which they developed a tropical depression. Once the trough phases were partitioned into various categories, any of the other three wave phases found within three data points (7.5°) east or west of each wave trough were considered to be part of that wave and used in the composites.

The Lightning Imaging Sensor (LIS) on board TRMM consists of an optical imager capable of recording brief radiance events associated with lightning (Christian et al. 1992; Boccippio et al. 2002) with an estimated detection efficiency of 70%–90% (Christian 1999;

188 Boccippio et al. 2000, 2002; no correction for detection efficiency was utilized for this study). In
189 particular, we used the 0.5° LIS flash counts and view time data to compute the daily lightning
190 flash density for 2.5° grid boxes (total flash count divided by view time over the area of a 2.5°
191 grid box).

192 The PR is a phased array radar system operating at 13.8 GHz (Kummerow et al. 1998;
193 Kozu et al. 2001). Specifically, attenuation-corrected radar reflectivity (Iguchi et al. 2000;
194 Meneghini et al. 2000; Iguchi et al. 2009) and a convective/stratiform classification (Awaka et al.
195 1998, 2009) from the PR 2A25 V6.0 product were utilized for this study. The reflectivity values
196 classified as convective were used to calculate mean convective reflectivity profiles for each 2.5°
197 box with 1-km height resolution from 1−18 km above ground level. Only convective rays of
198 data with a rain bottom below 2 km and not classified as warm rain were used in the construction
199 of these mean profiles to isolate the type of convection presumably most relevant for tropical
200 cyclogenesis.

201 The convective rain classification from 2A25 V6.0 was also used to tabulate the
202 percentage convective coverage over each 2.5° box. Another coverage parameter was calculated
203 using data from the 4-km NASA global-merged IR brightness temperature dataset (Liu et al.
204 2009). Specifically, the fractional coverage by IR brightness temperatures ≤210 K and ≤240 K
205 over each 2.5° box was calculated to examine the coverage by cold cloudiness.

206 The TMI instrument is a nine-channel passive microwave radiometer (Kummerow et al.
207 1998). Four TMI channels were used in this study, including the 37.0 GHz and 85.5 GHz
208 horizontally- and vertically-polarized channels. The measured radiances in these channels are
209 especially sensitive to scattering by ice (e.g., Spencer et al. 1989; Smith et al. 1992; Cecil and
210 Zipser 1999; Toracinta et al. 2002). Significant scattering and an accompanying reduction in the

measured brightness temperatures at 85.5 GHz can be accomplished by relatively small ice particles (~10^{-4} m in diameter), but significant reductions in brightness temperatures at 37.0 GHz require the presence of larger (millimeter-sized) particles (Toracinta et al. 2002). Therefore, a significant reduction in 37.0-GHz brightness temperatures likely indicates a stronger updraft and more intense convection required for the formation and maintenance of large ice particles in the upper portions of clouds. The 85.5-GHz channel has also been used in several earlier studies to characterize the intensity and spatial extent of convection (e.g., Mohr and Zipser 1996; Cecil and Zipser 1999; Mohr et al. 1999).

At 37.0 and 85.5 GHz, variations in surface emissivity and temperature can lead to large variations in brightness temperature unrelated to the overlying atmosphere. To remove these variations, we combined temperatures measured from both 85.5-GHz channels into 85.5-GHz polarization corrected temperatures (PCT_{85}) as defined by Spencer et al. (1989). Similarly, the two 37.0-GHz channels were combined to form PCT_{37} as defined by Toracinta et al. (2002) and Cecil et al. (2002). Cecil and Zipser (2002) found that vigorous convection was generally present when PCT_{85} were below ~200 K and PCT_{37} were below ~263 K. Hence, only TMI pixels with $PCT_{85} \leq 200$ K and $PCT_{37} \leq 260$ K were used to calculate an average PCT_{85} and PCT_{37} over each 2.5° box.

Lightning flash rates, mean convective reflectivity profiles, mean PCTs, percentage convective coverage values, and IR fractional coverage values were subsequently composited as a function of wave phase for the different wave types over the various longitude bands (Fig. 1). Note that some developing wave composites were not created over every longitude band because after initial tropical cyclone development, developing waves were no longer tracked. For example, composites were created for waves which spawn tropical cyclones over the East

Atlantic (i.e., East Atlantic developing waves; EADWs) over only the Africa and East Atlantic longitude bands. EADWs were tracked up until they developed cyclones over the East Atlantic but not farther west.

The parameters we analyze here basically relate to either the areal coverage of convection (percentage convective coverage, coverage below IR brightness temperature thresholds) or the vigor of convection that does occur (lightning flash rate, mean PCTs for pixels below certain thresholds, mean convective reflectivity). The IR thresholds (210 K and 240 K) go beyond characterizing the convective area as cold anvils expand. Flash rate is somewhat related to both the coverage and intensity of convection, but one or more elements of intense convection can dominate this parameter much more than a large number of weak convective cells would. The PCT thresholds used here restrict the analysis to only pixels related to strong, deep convection. Hence, our mean PCT values are indicative of how strong that convection is when it does occur. (Note that taking the mean PCT without using thresholds [not shown] would be more related to the rain area and would be quite different than the mean PCTs with thresholds.) Similarly, our mean reflectivity values consider only the pixels that are already classified as convective, so they relate to how strong that convection is.

In order to test whether values from developing waves and NDWs are significantly different, the analysis of variance statistical technique was used. This provides an estimate of the error variance associated with some group of data and an estimate of the systematic variance between groups of data. If the systematic variance is greater than the error variance, then the f-statistic is used to test whether the systematic effect is significantly greater than the random error effect. A significantly greater systematic effect suggests a high probability that differences between groups of data are, indeed, real and not just due to chance. Note for this study that a

difference is considered to be significant if the f-statistic indicates significance at or above the 99% level. Additional information on the analysis of variance technique can be found in Panofsky and Brier (1958).

3. Results

a. Comparison between East Atlantic Developing Waves and NDWs

Table 2 shows the number of distinct easterly waves and the number of individual data points included in the trough phase composites of various wave categories, including EADWs and NDWs. Note that as a result of wave merger/splitting as well as the ambiguities associated with counting weak NDWs that alternately can be tracked for a short time over the analysis domain and then become too weak to be tracked, the number of distinct NDWs in Table 2 is only an estimate.

The composite coverage by IR brightness temperature thresholds are provided in Table 3 over various longitude bands for various wave categories, including for EADWs and NDWs. Over Africa, the coverage by temperatures $\leq$210 K and $\leq$240 K is significantly greater in all EADW phases (except for the 210 K threshold in the trough phase) compared to the corresponding NDW values. Over the East Atlantic, significantly greater EADW values are confined to only the trough and northerly phases. Similarly, the composite percentage convective coverage values for EADWs and NDWs in Table 4 indicate that coverage is greater for EADWs over both Africa and the East Atlantic in each wave phase, except the ridge phase over the East Atlantic. The differences between EADWs and NDWs in the northerly phase over both Africa and the East Atlantic are significant, and the difference between trough phase values over the East Atlantic is also relatively large (while not significant at the 99% level, it is

284 significant at the 95% level). Thus, as EADWs approach their genesis region over the East
285 Atlantic, the maximum convective and cold cloudiness coverage occurs ahead of and within the
286 wave trough where it may interact with the larger-scale wave helping to amplify the wave,
287 perhaps making it more favorable for cyclogenesis (LP10).

288 While the differences in composite lightning flash rates (Table 5) between EADWs and
289 NDWs over Africa are not significant at the 99% level, all EADW phases, except the trough, are
290 associated with significantly higher flash rates than the corresponding NDW phases valid at the
291 95% level. The trough value is similar for EADWs and NDWs over Africa. Consistent with
292 several previous studies which show a decrease in lightning over the ocean compared to land
293 (e.g., Christian et al. 2003), lightning decreases substantially over the East Atlantic compared to
294 Africa. Nevertheless, except in the southerly phase, all EADW flash rates over the East Atlantic
295 are greater than those of NDWs. But, these differences are relatively small (i.e., not significant
296 at the 99% level). Thus, the lightning data suggest that EADWs are generally associated with
297 more vigorous convection than that of NDWs.

298 Table 6 shows PCT_{37} and PCT_{85} values as a function of wave phase for various wave
299 types and regions. Differences between EADWs and NDWs over both Africa and the East
300 Atlantic are quite small and are not significant in any phase. Nevertheless, EADW values are
301 generally slightly less than those of NDWs over both regions, suggesting a slightly stronger ice
302 scattering signature and somewhat more vigorous convection for EADWs.

303 The difference between mean convective reflectivity values of EADWs and NDWs
304 (EADW minus NDW values) as a function of wave phase valid over the East Atlantic is shown
305 in Fig. 2. Note that differences are calculated and shown in Fig. 2 and all subsequent figures
306 only where the mean reflectivity values for both developing waves and NDWs are ≥18 dBZ (the

approximate minimum detectable signal of the PR; Yang et al. 2006). Differences are generally positive in Fig. 2, indicating greater reflectivity values for EADWs. These larger reflectivity values would presumably be associated with stronger updrafts and more vigorous convection in order to support such reflectivity values. However, only the value at 2.5 km in the northerly phase and 4.5–5.5 km in the southerly phase are significantly greater for EADWs (indicated by squares in Fig. 2). Thus, considering how many levels and phases fail the significance tests, we cannot infer much from the few levels that do show significance. In addition, the differences between EADW and NDW reflectivity profiles over Africa (not shown) are also small and not statistically significant.

In summary, EADWs appear to be associated with a greater *coverage* by convection and cold cloudiness over both Africa and the East Atlantic compared to NDWs. There is only slight indication of more intense convection associated with EADWs. These results are generally consistent with the results of LP10 where developing waves were found to be associated with a greater coverage by cold cloud tops and more lightning compared to NDWs. The coverage by IR brightness temperatures $\leq$240 K and/or $\leq$210 K provide the greatest number of statistically significant differences between EADWs and NDWs over both Africa and the East Atlantic, thus, providing the best discrimination between EADWs and NDWs.

Some waves included in the NDW composite are associated with relatively little cold cloudiness and convection and, from an operational forecasting perspective, would clearly be distinguished from developing waves. Hence, a comparison between these NDWs and developing waves is not particularly instructive. To make a comparison between developing waves and NDWs associated with a similar probability of development, the archived Graphical Tropical Weather Outlooks produced by the NHC were examined in order to identify easterly

waves that were assigned a moderate (30−50%) chance of genesis within 48 hours. Composites were created for NDWs and all developing waves in 2009 and 2010 (the archived outlooks were only available for the last two years of the study) at the times and locations when these waves were assigned a 30−50% chance of genesis by the NHC. Forty-two (117) distinct easterly waves (individual trough data points) were included in these developing wave composites. Note that 40 of these 42 waves actually developed within 48 hours. Nine (42) distinct waves (trough points) were included in the NDW composites. Table 7 shows the statistics for these 30−50% chance-of-genesis developing and NDW composites valid over the full analysis domain (to maximize the sample size). Coverage by IR brightness temperatures ≤240 K, convective coverage, and flash rates are greater in nearly all developing wave phases compared to the corresponding NDW phases with the greatest differences generally found in the trough and northerly phases. In addition, PCT_{37} values are smaller in all developing wave phases, except the southerly phase. Therefore, when developing and NDWs were associated with an enhanced probability of cyclogenesis according to the NHC, developing waves appear to be associated with more widespread and intense convection, in general, in agreement with the results of the comparison between all NDWs and EADWs. Note that none of the variables show statistically significant differences between developing waves and NDWs associated with a moderate probability of genesis, possibly due to relatively small sample sizes.

The climatological peak of tropical cyclone occurrence in the Atlantic occurs around August–September (e.g., Landsea 1993). Hence, we wanted to examine possible intra-seasonal impacts on our results by examining a comparison between EADWs and NDWs valid only for August–September. In general, this comparison (not shown) revealed patterns similar to those found for the comparison valid for June–November, especially over the East Atlantic (i.e.,

353 greater coverage and/or intensity of convection for EADWs). However, the magnitude of
354 differences between the two wave categories valid for the shortened time period were somewhat
355 smaller and less often statistically significant than observed for the comparison valid for the full
356 time period. Restricting the NDW composite to those waves that occur in August−September
357 may lead to a composite of waves that presumably propagate through an environment
358 climatologically more favorable for cyclogenesis (e.g., moister environment) and for more
359 widespread/intense convection compared to the full June–November sample.
360
361 *b. Comparison between West Atlantic – Caribbean Developing Waves and NDWs*
362
363
364 In order to increase the sample size (Table 2), waves that developed a tropical cyclone
365 over either the West Atlantic or Caribbean were combined into a single category (i.e., West
366 Atlantic − Caribbean developing waves; WACDWs). The coverage by certain IR thresholds
367 shown in Table 3 indicate that WACDWs are associated with significantly greater coverage by
368 cold cloud tops compared to NDWs in all phases except the ridge over Africa, the West Atlantic,
369 and the Caribbean. WACDW ridge values over these regions are also greater than those of
370 NDWs, but not with 99% level significance. Over the East Atlantic, only the coverage by cold
371 cloud tops in the trough phase is significantly greater for WACDWs. The coverage by cold
372 cloudiness in other WACDW phases over the East Atlantic is generally less than the
373 corresponding NDW values (the 240 K threshold in the southerly phase is actually significantly
374 less). Thus, a persistent large coverage by cold cloudiness in the trough phase may be important
375 for the genesis of tropical cyclones from WACDWs, while coverage by cold cloud tops in the
376 ridge phase is relatively unimportant for genesis.

377 The percentage convective coverage values shown for WACDWs and NDWs in Table 4
378 indicate few significant differences between the two wave categories over any longitude band.
379 In fact, only the WACDW trough over the West Atlantic is associated with significantly more
380 convective coverage than the NDW trough. The coverage in the WACDW northerly phase over
381 the Caribbean is also much greater than the corresponding NDW value, but the difference is only
382 significant at the 95% level. Despite the relative lack of statistically significant differences,
383 convective coverage is greater in all WACDW phases over Africa, the West Atlantic, and the
384 Caribbean (except for the ridge over Africa and trough over the Caribbean). Over the East
385 Atlantic, coverage in the WACDW trough and ridge is greater than the corresponding NDW
386 values, while northerly and southerly values are nearly identical between the two wave
387 categories over this band. Thus, convective coverage is generally larger for WACDWs over all
388 longitude bands, especially as these waves approach their genesis region over either the West
389 Atlantic or Caribbean.
390 None of the WACDW lightning flash rates are significantly different from those of
391 NDWs (Table 5) over any longitude band. However, over Africa and the Caribbean, flash rates
392 for all WACDW phases are greater than the corresponding NDW values. Flash rates over the
393 East and West Atlantic are also generally slightly greater for WACDWs. The mean PCTs from
394 deep convection in WACDWs (Table 6) also suggest no significant differences between
395 WACDW and NDW values with some values slightly greater for WACDWs and others slightly
396 greater for NDWs. Hence, the intensity of convection associated with WACDWs as indicated by
397 lightning and low PCTs does not appear to be all that different from that of NDWs.
398 The differences between mean vertical profiles of convective reflectivity for WACDWs
399 and NDWs as a function of wave phase over various longitude bands are shown in Fig. 3. Very

few of the differences between WACDWs and NDWs are significant. Only values at 3.5–4.5 km in the northerly phase over the Caribbean and 3.5–5.5 km in the trough over the West Atlantic are significantly greater for WACDWs. Despite the lack of significant differences, reflectivity values are greater for WACDWs at all heights in all phases, except the ridge, as these waves approach their genesis region over the Caribbean. In contrast, over Africa, NDWs are generally associated with greater reflectivity values in all phases, except the northerly phase. Hence, as WACDWs move from their origin over Africa to where they develop tropical cyclones over the West Atlantic and Caribbean, convective reflectivity values associated with these waves generally increase slightly relative to NDWs.

Similar to EADWs, the coverage by cold cloudiness (i.e., using IR thresholds) provides the greatest number of statistically significant differences between WACDWs and NDWs and appears to be the best discriminator between these two wave types, especially within the trough phase. While convective coverage, lightning flash rates, mean cold PCTs, and convective reflectivity provide few statistically significant differences between WACDWs and NDWs, these variables appear to indicate that WACDWs are associated with a greater coverage and intensity of convection as these waves approach their genesis region. This enhancement of convection associated with WACDWs may help to moisten the larger-scale waves at mid/upper levels (e.g., Dunkerton et al. 2009) and/or increase larger-scale mid to low-level vorticity (e.g., Montgomery et al. 2006; Nolan 2007; Raymond et al. 2011), helping to create an environment more favorable for tropical cyclogenesis.

A comparison was also made between WACDWs and NDWs valid only for those months when WACDWs are most active (i.e., August–October) as indicated by the annual distribution of

WACDW data points (not shown). Similar to EADWs, the restricted WACDW comparison generally did not change the results obtained from the full June–November comparison.

c. Comparison between East Pacific Developing Waves and NDWs

Waves that developed tropical cyclones over the East Pacific (i.e., East Pacific developing waves; EPDWs) are obviously a long distance from where they develop tropical cyclones while the waves are near their origin over Africa, and there are several complicating factors (e.g., topography of Central America; Zehnder 1991; Mozer and Zehnder 1996; Farfan and Zehnder 1997; Zehnder et al. 1999; barotropic instability over the Caribbean and East Pacific; Molinari et al. 1997) that could influence an EPDW between Africa and the East Pacific. Hence, convection over Africa would not be expected to exert much of an influence on later tropical cyclogenesis over the East Pacific. Nevertheless, EPDW lightning flash rates and coverage by cold cloudiness valid for June–November (not shown) are significantly *greater* than corresponding NDW values in various wave phases over Africa. However, the June–November NDW composite over Africa includes all waves, including those waves that were too weak to track all the way across the Atlantic and waves with relatively little convection. A comparison between EPDW and NDW composites valid for only July and August (two of the most active months for tropical cyclogenesis in the East Pacific), which restricts the NDW composite to those waves that presumably move through an environment climatologically more favorable for convection and for cyclogenesis, shows a much different pattern than that observed for June–November. For example, the coverage by IR brightness temperatures below certain thresholds over Africa valid for July–August only (Table 8) shows *smaller* EPDW coverage in all phases (240 K threshold differences are significant in every phase, except the ridge phase, while 210 K

differences are significant in the trough and northerly phases) compared to the corresponding NDW values. Thus, the focus of this subsection will be on a comparison between EPDWs and NDWs valid for July–August because this restricted comparison appears to provide more meaningful results than those obtained from the June–November comparison.

As EPDWs move over the East and West Atlantic, the coverage by cold cloudiness (Table 8) becomes comparable to that of NDWs with some values greater for EPDWs and other values greater for NDWs with no significant differences. Over the Caribbean and East Pacific, all IR threshold coverage values are greater for EPDWs. Values are significantly greater in the EPDW southerly phase over the Caribbean and all phases over the East Pacific (except for the 210 K value in the ridge). Convective coverage (not shown) is generally greater for NDWs over Africa, the East Atlantic, and West Atlantic, but differences between these waves and EPDWs are generally not significant. In contrast, convective coverage is often greater for EPDWs over the Caribbean and East Pacific with significantly greater values in the southerly phase over the Caribbean and northerly and southerly phases over the East Pacific. Thus, relative to NDWs, convective and cold cloudiness coverage is smaller for EPDWs over Africa and generally increases as EPDWs move across the Atlantic and approach their genesis region.

Composite lightning flash rates for EPDWs and NDWs (Table 9) indicate that flash rates are smaller in all EPDW phases over Africa compared to the corresponding NDW values, but differences are not significant. Over the East Atlantic, West Atlantic, and Caribbean, flash rates are comparable between EPDWs and NDWs with some values greater for EPDWs and others greater for NDWs. When EPDWs are over the East Pacific where they develop tropical cyclones, flash rates in all phases of these waves are greater (significantly greater in all but the ridge phase) than the corresponding NDW values.

A comparison between EPDW and NDW cold PCTs (not shown) indicates, similar to other developing waves, little difference between the two wave types. However, over the East Pacific, EPDW trough and southerly phase PCT_{85} values are significantly less than the corresponding NDW values, suggesting more intense convection for these waves near their genesis region. Overall, though, differences between developing waves (EADWs, WACDWs, and EPDWs) and NDWs in terms of mean cold PCTs are quite small over all longitude bands, suggesting that this way of comparing PCTs (taking the mean of pixels below a threshold for deep convection) may not be the best use of passive microwave information.

Over all longitude bands east of the East Pacific band, differences between EPDWs and NDWs in terms of mean convective reflectivity profiles (not shown) are generally small with few statistically significant differences. Differences in convective reflectivity profiles between EPDWs and NDWs over the East Pacific (Fig. 4) indicate generally greater values for EPDWs in all phases at all levels. EPDW values are significantly greater between 2.5 and 5.5 km in the northerly phase, at 2.5 km in the trough, and at 3.5 km in the southerly phase. Thus, when EPDWs are near their origin over Africa, differences between these waves and NDWs in terms of convective reflectivity are small. Differences remain small until EPDWs move over their genesis region of the East Pacific, where low- to mid-level reflectivity values become significantly greater for these waves in all phases other than the ridge.

In summary, EPDW convective coverage and/or intensity appear to be relatively low compared to NDWs near their origin over Africa. As EPDWs move across the Atlantic, Caribbean, and into the East Pacific region, convective coverage and/or intensity gradually become significantly greater than that of NDWs. The pronounced increase in convection over the Caribbean and East Pacific may be related to barotropic instability found over these regions

493 (Molinari et al. 1997). It is possible that this instability over the Caribbean and East Pacific
494 could help amplify easterly waves, perhaps helping to spawn more convection within the waves
495 over these regions. In addition, the Caribbean region may be associated with an enhancement of
496 convection due to the large landmasses in that region (cf. Fig. 1). Note that both EPDWs and
497 NDWs are subject to the effects of land and its associated diurnal cycle of convection over the
498 Caribbean region. Thus, any differences observed between these two wave types in terms of
499 characteristics of convection should not be due to land/ocean differences.

500 In contrast to EADWs and WACDWs where the coverage by IR thresholds was clearly
501 the one variable that could provide the best discrimination between these waves and NDWs,
502 several variables could potentially be used to separate EPDWs from NDWs over the East Pacific,
503 including IR thresholds, lightning flash rates, and low-level PR convective reflectivity values.
504 This may suggest that the coverage and intensity of convection over the East Pacific are
505 important for tropical cyclogenesis over this region.

506 Based on NHC (2011), some waves spawned a tropical cyclone in both the Atlantic and
507 East Pacific basins. To determine if there were any differences in terms of convective
508 characteristics between these waves which spawned multiple cyclones and those which spawned
509 only one storm, composites were created for waves that developed multiple cyclones. However,
510 few significant differences were found between multiple and single cyclone waves. Waves
511 which develop multiple cyclones may lend themselves better to case study analysis which is left
512 for future work.

513 Again using information from NHC (2011), developing waves were also separated
514 according to whether the subsequent tropical cyclone achieved hurricane strength or only tropical
515 storm strength. Composites were also created for both of these wave categories. Except for

some differences between hurricane and tropical storm waves over the West Atlantic, the convective characteristics of hurricane and tropical storm waves are generally not significantly different. These results are not surprising because many other factors (e.g., SSTs, wind shear) help control the final strength of a tropical cyclone. In addition, because we are not controlling for large-scale conditions, the relative enhancement of convection in hurricane waves over the West Atlantic could be a result of large-scale conditions favorable for both convection and intensification to hurricane strength. In this case, the enhanced convection in the precursor wave is not a factor responsible for intensification to hurricane strength.

4. Summary and Conclusions

This study examines the characteristics of convection and cold cloudiness associated with tropical easterly waves using data from the Tropical Rainfall Measurement Mission (TRMM) Lightning Imaging Sensor, Precipitation Radar (PR), and Microwave Imager as well as IR brightness temperatures from the NASA global-merged dataset. In particular, the purpose of the study was to determine which characteristics or observations of convection provide the best distinction between developing waves and nondeveloping waves (NDWs) and over which regions. Another goal of the study was to determine whether the convective characteristics that provide the best distinction between the two wave types vary for waves that develop tropical cyclones over different regions.

Results suggest that the variables that provide the best distinction between developing waves and NDWs do vary between the Atlantic and East Pacific. In particular, the coverage by IR brightness temperatures $\leq$240 K and $\leq$210 K appear to provide the largest distinction between East Atlantic developing waves (EADWs; waves which developed a tropical cyclone over the

East Atlantic) and NDWs in all wave phases over Africa and in the trough and northerly phases over the East Atlantic. The coverage by IR thresholds also provides the best distinction between West Atlantic – Caribbean developing waves (WACDWs; waves which spawned a cyclone over either the West Atlantic or Caribbean) and NDWs. In particular, the coverage by cold cloudiness was found to be significantly greater for WACDWs in all phases, except the ridge, over all longitude bands but the East Atlantic (values are only significantly greater for WACDWs in the trough over the East Atlantic). Thus, results for WACDWs indicate that a persistent large coverage by cold cloudiness in the trough phase may be important for cyclogenesis from these waves. The fact that indices of the coverage by convection/cold cloudiness provide a better discrimination between developing waves over the Atlantic and NDWs than indicators of convective intensity (e.g., lightning flash rates, polarization corrected temperatures) suggests that the coverage by convection is more important than intensity for tropical cyclogenesis over the Atlantic.

In contrast to waves which developed a tropical cyclone over the Atlantic basin, waves which spawned a tropical cyclone over the East Pacific (East Pacific developing waves; EPDWs) are associated with statistically significantly greater IR threshold coverage, convective coverage, lightning flash rates, and low-level PR convective reflectivity in various wave phases (no clear preference for enhanced convection in any one wave phase over another) when compared to NDWs over the East Pacific. In contrast to what was found for EADWs and WACDWs, restricting the comparison between EPDWs and NDWs to only the most active months for East Pacific cyclogenesis led to quite different results from the corresponding comparison valid for June−November, especially over Africa. This suggests that care must be taken in selecting a

temporal domain for a comparison between EPDWs and NDWs and/or selecting a sample of NDWs.

Future work could involve developing thresholds based on the most relevant convective parameters to help provide an indication of enhanced probability (or lack thereof) of tropical cyclogenesis. For example, Table 10 lists the most relevant parameters for EADWs, WACDWs, and EPDWs over various regions and initial thresholds that could be tested for each parameter. These thresholds are based approximately on the 99% significance level for the sample sizes used for this study. Other future work could involve incorporating these convective indicators that provide the greatest distinction between developing waves and NDWs in the development of a statistical cyclogenesis/hurricane prediction model.

Acknowledgements.

This work was part of the lead author's research for his doctoral degree, and funding for the research was provided through a NASA Earth and Space Science Fellowship, Grant #NNX09AO40H. Dr. Walter Petersen and Dr. Daniel Cecil also acknowledge funding from the NASA PMM/TRMM Program. Suggestions from Dr. Ron McTaggart-Cowan and two anonymous reviewers greatly improved an earlier version of this manuscript. The authors would also like to gratefully acknowledge the Goddard Earth Sciences Data and Information Services Center for providing the TMI, PR, and IR brightness temperature data, the NASA EOSDIS Global Hydrology Resource Center DAAC for providing the LIS science data, and the NOAA/OAR/ESRL PSD for providing the NCEP-NCAR reanalysis data.

REFERENCES

Avila, L. A., 1991: Eastern North Pacific hurricane season of 1990. *Mon. Wea. Rev.*, **119**, 2034−2046.

_____, and R. J. Pasch, 1992: Atlantic tropical systems of 1991. *Mon. Wea. Rev.*, **120**, 2688−2696.

Awaka, J., T. Iguchi, and K. Okamoto, 1998: Early results on rain type classification by the Tropical Rainfall Measuring Mission (TRMM) precipitation radar. *Proc. Eighth URSI Commission F. Triennial Open Symp.*, Aveiro, Portugal, International Union of Radio Science, 143–146.

_____, _____, and _____, 2009, TRMM PR standard algorithm 2A23 and its performance on bright band detection. *J. Meteor. Soc. Japan*, **87A**, 31–52.

Berry, G. J., and C. Thorncroft, 2005: Case study of an intense African easterly wave. *Mon. Wea. Rev.*, **133**, 752–766.

Boccippio, D. J., S. J. Goodman, and S. Heckman, 2000: Regional differences in tropical lightning distributions. *J. Appl. Meteor.*, **39**, 2231–2248.

_____, W. J. Koshak, and R. J. Blakeslee, 2002: Performance assessment of the optical transient detector and lightning imaging sensor. Part I: Predicted diurnal variability. *J. Atmos. Oceanic Technol.*, **19**, 1318–1332.

Bracken, W. E., and L. F. Bosart, 2000: The role of synoptic-scale flow during tropical cyclogenesis over the North Atlantic Ocean. *Mon. Wea. Rev.*, **128**, 353–376.

Burpee, R. W., 1972: The origin and structure of easterly waves in the lower troposphere of North Africa. *J. Atmos. Sci.*, **29**, 77–89.

610 _____, 1974: Characteristics of North African easterly waves during the summers of 1968 and
611 1969. *J. Atmos. Sci.*, **31**, 1556–1570.
612 Carlson, T. N., 1969: Synoptic histories of three African disturbances that developed into
613 Atlantic hurricanes. *Mon. Wea. Rev.*, **97**, 256–276.
614 Cecil, D. J., and E. J. Zipser, 1999: Relationships between tropical cyclone intensity and
615 satellite-based indicators of inner core convection: 85-GHz ice-scattering signature and
616 lightning. *Mon. Wea. Rev.*, **127**, 103–123.
617 _____, _____, and S. W. Nesbitt, 2002: Reflectivity, ice scattering, and lightning
618 characteristics of hurricane eyewalls and rainbands. Part I: Quantitative description. *Mon.*
619 *Wea. Rev.*, **130**, 769–784.
620 _____, and _____, 2002: Reflectivity, ice scattering, and lightning characteristics of hurricane
621 eyewalls and rainbands. Part II: Intercomparison of observations. *Mon. Wea. Rev.*, **130**,
622 785–801.
623 Christian, H. J., R. J. Blakeslee, and S. L. Goodman, 1992: Lightning Imaging Sensor (LIS) for
624 the Earth Observing System. NASA TM-4350, 36 pp.
625 _____, 1999: *Atmospheric Electricity*, Guntersville, AL, NASA/CP-1999-209261, 715–718.
626 _____, and Coauthors, 2003: Global frequency and distribution of lightning as observed from
627 space by the optical transient detector. *J. Geophys. Res.*, **108**, 4005,
628 doi:10.1029/2002JD002347.
629 Chronis, T. G., E. R. Williams, E. N. Anagnostou, and W. A. Petersen, 2007: African lightning:
630 Indicator of tropical Atlantic cyclone formation. *Eos, Trans. Amer. Geophys. Union*, **88**,
631 397–398.

Deierling, W., and W. A. Petersen, 2008: Total lightning activity as an indicator of updraft characteristics. *J. Geophys. Res.*, **113**, D16210, doi:10.1029/2007JD009598.

Dunkerton, T. J., M. T. Montgomery, and Z. Wang, 2009: Tropical cyclogenesis in a tropical wave critical layer: Easterly waves. *Atmos. Chem. Phys.*, **9**, 5587–5646.

Duvel, J-Ph., 1990: Convection over tropical Africa and the Atlantic Ocean during northern summer. Part II: Modulation by easterly waves. *Mon. Wea. Rev.*, **118**, 1855–1868.

Farfan, L. M., and J. A. Zehnder, 1997: Orographic influence on the synoptic-scale circulations associated with the genesis of Hurricane Guillermo (1991). *Mon. Wea. Rev.*, **125**, 2683−2698.

Gray, W. M., 1968: Global view of the origin of tropical disturbances and storms. *Mon. Wea. Rev.*, **96**, 669–700.

Gu, G., R. F. Adler, G. J. Huffman, and S. Curtis, 2004: African easterly waves and their association with precipitation. *J. Geophys. Res.*, **109**, D04101, doi:10.1029/2003/JD003967.

Hendricks, E. A., M. T. Montgomery, and C. A. Davis, 2004: The role of "vortical" hot towers in the formation of tropical cyclone Diana (1984). *J. Atmos. Sci.*, **61**, 1209–1232.

Hopsch, S. B., C. D. Thorncroft, and K. R. Tyle, 2010: Analysis of African easterly wave structures and their role in influencing tropical cyclogenesis. *Mon. Wea. Rev.*, **138**, 1399–1419.

Houze, R. A., Jr., W.-C. Lee, and M. M. Bell, 2009: Convective contribution to the genesis of Hurricane Ophelia (2005). *Mon. Wea. Rev.*, **137**, 2778−2800.

Iguchi, T., T. Kozu, R. Meneghini, J. Awaka, and K. Okamoto, 2000: Rain-profiling algorithm for the TRMM precipitation radar. *J. Appl. Meteor.*, **39**, 2038–2052.

_____, _____, J. Kwiatkowski, R. Meneghini, J. Awaka, and K. Okamoto, 2009: Uncertainties in the rain profiling algorithm for the TRMM precipitation radar. *J. Meteor. Soc. Japan*, **87A**, 1–30.

Kalnay, E., and Coauthors, 1996: The NCEP/NCAR 40-year reanalysis project. *Bull. Amer. Meteor. Soc.*, **77**, 437–471.

Kozu, T., and Coauthors, 2001: Development of precipitation radar onboard the Tropical Rainfall Measuring Mission (TRMM) satellite. *IEEE Trans. Geosci. Remote Sens.*, **39**, 102−116.

Kummerow, C., W. Barnes, T. Kozu, J. Shiue, and J. Simpson, 1998: The tropical rainfall measuring mission (TRMM) sensor package. *J. Atmos. Oceanic Technol.*, **15**, 809–817.

Kurihara, Y., and R. E. Tuleya, 1981: A numerical simulation study on the genesis of a tropical storm. *Mon. Wea. Rev.*, **109**, 1629–1653.

Landsea, C. W., 1993: A climatology of intense (or major) Atlantic hurricanes. *Mon. Wea. Rev.*, **121**, 1703–1713.

_____, G. D. Bell, W. M. Gray, and S. B. Goldenberg, 1998: The extremely active 1995 Atlantic hurricane season: Environmental conditions and verification of seasonal forecasts. *Mon. Wea. Rev.*, **126**, 1174–1193.

Leary, L. A., and E. A. Ritchie, 2009: Lightning flash rates as an indicator of tropical cyclone genesis in the Eastern North Pacific. *Mon. Wea. Rev.*, **137**, 3456–3470.

Leppert, K. D., II, and W. A. Petersen, 2010: Electrically-active hot towers in African easterly waves prior to tropical cyclogenesis. *Mon. Wea. Rev.*, **138**, 663−687.

_____, and D. J. Cecil, 2012: African easterly wave convection and tropical cyclogenesis: A Lagrangian perspective. *Extended Abstracts, 30th Conf. on Hurricanes and Tropical Meteorology*, Ponte Vedra Beach, FL, Amer. Meteor. Soc., 3C.6.

Liu, Z., D. Ostrenga, G. G. Leptoukh, and A. V. Mehta, 2009: Online visualization and analysis of global half-hourly pixel-resolution infrared dataset. *Extended Abstracts, 25th Conf. on International Interactive Information and Processing Systems (IIPS) for Meteorology, Oceanography, and Hydrology*, Phoenix, AZ, Amer. Meteor. Soc., J3.4.

Meneghini, R., T. Iguchi, T. Kozu, L. Liao, K. Okamoto, J. A. Jones, and J. Kwiatkowski, 2000: Use of the surface reference technique for path attenuation estimates from the TRMM precipitation radar. *J. Appl. Meteor.*, **39**, 2053–2070.

Mohr, K. I., and E. J. Zipser, 1996: Defining mesoscale convective systems by their 85-GHz ice-scattering signatures. *Bull. Amer. Meteor. Soc.*, **77**, 1179–1189.

_____, J. S. Famiglietti, and E. J. Zipser, 1999: The contribution to tropical rainfall with respect to convective system type, size, and intensity estimated from the 85-GHz ice-scattering signature. *J. Appl. Meteor.*, **38**, 596–606.

Molinari, J., and D. Vollaro, 2000: Planetary- and synoptic-scale influences on Eastern Pacific tropical cyclogenesis. *Mon. Wea. Rev.*, **128**, 3296–3307.

_____, D. Knight, M. Dickinson, D. Vollaro, and S. Skubis, 1997: Potential vorticity, easterly waves, and Eastern Pacific tropical cyclogenesis. *Mon. Wea. Rev.*, **125**, 2699−2708.

Montgomery, M. T., M. E. Nicholls, T. A. Cram, and A. B. Saunders, 2006: A vortical hot tower route to tropical cyclogenesis. *J. Atmos. Sci.*, **63**, 355–386.

Mozer, J. B., and J. A. Zehnder, 1996: Lee vorticity production by large-scale tropical mountain ranges. Part I: Eastern North Pacific tropical cyclogenesis. *J. Atmos. Sci.*, **53**, 521−538.

National Hurricane Center, cited 2011: NHC archive of hurricane seasons. [Available online at http://www.nhc.noaa.gov/pastall.shtml.]

Nolan, D. S., 2007: What is the trigger for tropical cyclogenesis? *Aust. Meteorol. Mag.*, **56**, 241–266.

Norquist, D. C., E. E. Recker, and R. J. Reed, 1977: The energetics of wave disturbances as observed during phase III of GATE. *Mon. Wea. Rev.*, **105**, 334–342.

Panofsky, H. A., and G. W. Brier, 1958: *Some applications of statistics to meteorology*. The Pennsylvania State University, 224 pp.

Petersen, W. A., R. Cifelli, D. J. Boccippio, S. A. Rutledge, and C. Fairall, 2003: Convection and easterly wave structures observed in the eastern Pacific warm pool during EPIC-2001. *J. Atmos. Sci.*, **60**, 1754–1773.

_____, and D. J. Boccippio, 2004: Variability of convective structure and lightning activity in tropical easterly waves. Preprints, *26th Conf. on Hurricanes and Tropical Meteorology*, Miami Beach, FL, Amer. Meteor. Soc.

Price, C., Y. Yair, and M. Asfur, 2007: East African lightning as a precursor of Atlantic hurricane activity. *Geophys. Res. Lett.*, **34**, L09805, doi:10.1029/2006GL028884.

Raymond, D. J., S. L. Sessions, and C. Lopez Carrillo, 2011: Thermodynamics of tropical cyclogenesis in the northwest Pacific. *J. Geophys. Res.*, **116**, D18101, doi:10.1029/2011JD015624.

Reasor, P. D., M. T. Montgomery, and L. F. Bosart, 2005: Mesoscale observations of the genesis of Hurricane Dolly (1996). *J. Atmos. Sci.*, **62**, 3151–3171.

720 Reed, R. J., D. C. Norquist, and E. E. Recker, 1977: The structure and properties of African
721 wave disturbances as observed during phase III of GATE. *Mon. Wea. Rev.*, **105**, 317–
722 333.
723 Ritchie, E. A., and G. J. Holland, 1997: Scale interactions during the formation of Typhoon
724 Irving. *Mon. Wea. Rev.*, **125**, 1377–1396.
725 Rotunno, R., and K. A. Emanuel, 1987: An air–sea interaction theory for tropical cyclones. Part
726 II: Evolutionary study using a non-hydrostatic axisymmetric numerical model. *J. Atmos.*
727 *Sci.*, **44**, 542–561.
728 Rutledge, S. A., E. R. Williams, and T. D. Keenan, 1992: The down under Doppler and
729 electricity experiment (DUNDEE): Overview and preliminary results. *Bull. Amer.*
730 *Meteor. Soc.*, **73**, 3–16.
731 Saunders, C. P. R., and S. L. Peck, 1998: Laboratory studies of the influence of the rime
732 accretion rate on charge transfer during crystal/graupel collisions. *J. Geophys. Res.*, **103**,
733 13949–13956.
734 Serra, Y. L., G. N. Kiladis, and M. F. Cronin, 2008: Horizontal and vertical structure of
735 easterly waves in the Pacific ITCZ. *J. Atmos. Sci.*, **65**, 1266–1284.
736 _____, _____, and K. I. Hodges, 2010: Tracking and mean structure of easterly waves over
737 the Intra-Americas Sea. *J. Climate*, **23**, 4823–4840.
738 Sippel, J. A., J. W. Nielsen-Gammon, and S. E. Allen, 2006: The multiple-vortex nature of
739 tropical cyclogenesis. *Mon. Wea. Rev.*, **134**, 1796–1814.
740 Smith, E. A., H. J. Cooper, X. Xiang, A. Mugnai, and G. J. Tripoli, 1992: Foundations for
741 statistical-physical precipitation retrieval from passive microwave satellite measurements.

Part I: Brightness temperature properties of a time-dependent cloud-radiation model. *J. Appl. Meteor.*, **31**, 506–531.

Spencer, R. W., H. M. Goodman, and R. E. Hood, 1989: Precipitation retrieval over land and ocean with the SSM/I: Identification and characteristics of the scattering signal. *J. Atmos. Oceanic Technol.*, **6**, 254–273.

Takahashi, T., 1978: Riming electrification as a charge generation mechanism in thunderstorms. *J. Atmos. Sci*., **35**, 1536-1548.

Thompson, R. M., S. W. Payne, E. E. Recker, and R. J. Reed, 1979: Structure and properties of synoptic-scale wave disturbances in the intertropical convergence zone of the eastern Atlantic. *J. Atmos. Sci.*, **36**, 53–72.

Thorncroft, C. D., N. M. J. Hall, and G. N. Kiladis, 2008: Three-dimensional structure and dynamics of African easterly waves. Part III: Genesis. *J. Atmos. Sci.*, **65**, 3596–3607.

Toracinta, E. R., D. J. Cecil, E. J. Zipser, and S. W. Nesbitt, 2002: Radar, passive microwave, and lightning characteristics of precipitating systems in the tropics. *Mon. Wea. Rev.*, **130**, 802–824.

Williams, E. R., S. A. Rutledge, S. G. Geotis, N. Renno, E. Rasmussen, and T. Rickenbach, 1992: A radar and electrical study of tropical "hot towers." *J. Atmos. Sci.*, **49**, 1386–1395.

Yang, S., W. S. Olson, J.-J. Wang, T. L. Bell, E. A. Smith, and C. D. Kummerow, 2006: Precipitation and latent heating distributions from satellite passive microwave radiometry. Part II: Evaluation of estimates using independent data. *J. Appl. Meteor. Climatol.*, **45**, 721–739.

Zehnder, J. A., 1991: The interaction of planetary-scale tropical easterly waves with topography: A mechanism for the initiation of tropical cyclones. *J. Atmos. Sci.*, **448**, 1217–1230.

765 _____, D. M. Powell, and D. L. Ropp, 1999: The interaction of easterly waves, orography, and
766 the intertropical convergence zone in the genesis of eastern Pacific tropical cyclones.
767 *Mon. Wea. Rev.*, **127**, 1566–1585.
768 Zipser, E. J., 1994: Deep cumulonimbus cloud systems in the tropics with and without lightning.
769 *Mon. Wea. Rev.*, **122**, 1837–1851.
770
771
772
773
774
775
776
777
778
779
780
781
782
783
784
785
786
787

List of Figures

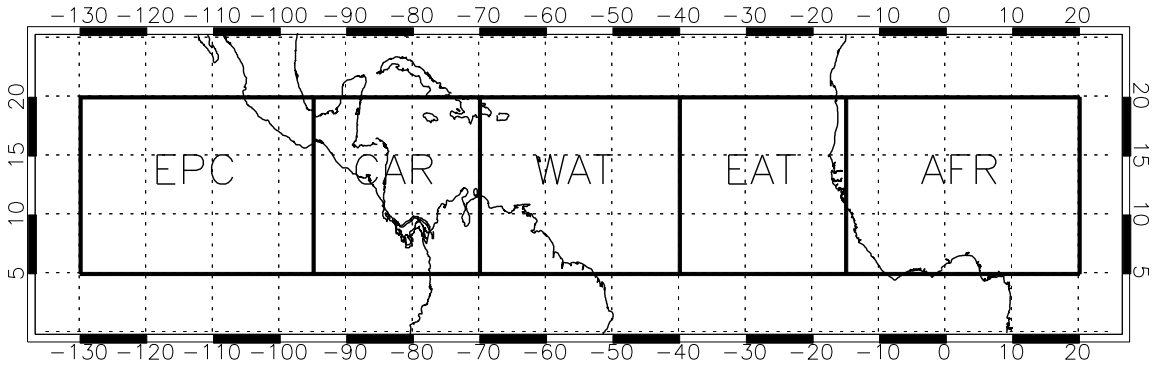

833

834 FIG. 1. Map showing the location of the full analysis domain (130°W–20°E) and smaller

835 longitude bands utilized for this study. EPC represents the East Pacific band, CAR the

836 Caribbean and Central America band, WAT the West Atlantic band, EAT the East Atlantic band,

837 and AFR the Africa longitude band.

838

839

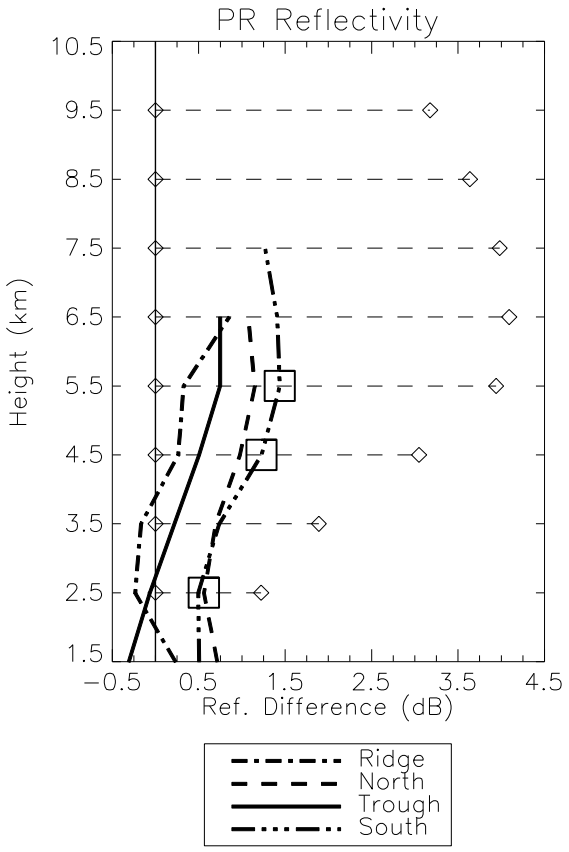

840

841 FIG. 2. Precipitation Radar (PR) convective reflectivity (only values classified as convective are
842 used) differences between East Atlantic developing waves (EADWs) and nondeveloping waves
843 (NDWs; i.e., EADW minus NDW values) as a function of height and wave phase *valid over the*
844 *East Atlantic*. The dashed horizontal lines depict the value of half the standard deviation at each
845 height, and the squares indicate EADW values that are significantly greater than the
846 corresponding values of NDWs valid at the 99% level.

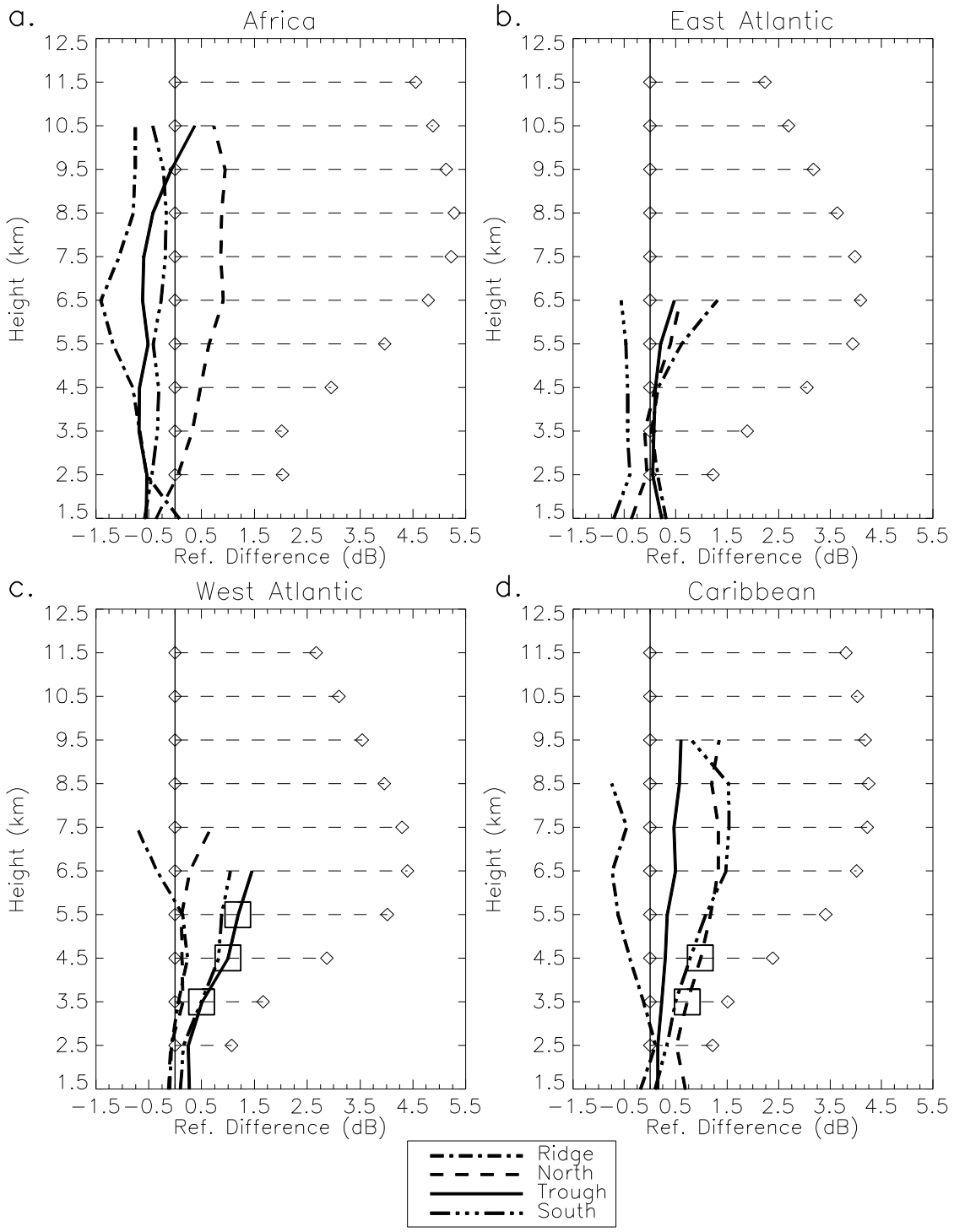

847

848 FIG. 3. Precipitation Radar convective reflectivity (only values classified as convective are used)

849 differences between West Atlantic – Caribbean developing waves (WACDWs) and

nondeveloping waves (NDWs; i.e., WACDW minus NDW values) as a function of height and wave phase *valid over* a.) *Africa* b.) *the East Atlantic* c.) *the West Atlantic,* and d.) *the Caribbean*. The dashed horizontal lines depict the value of half the standard deviation at each height, and the squares indicate WACDW values that are significantly greater than the corresponding NDW values valid at the 99% level.

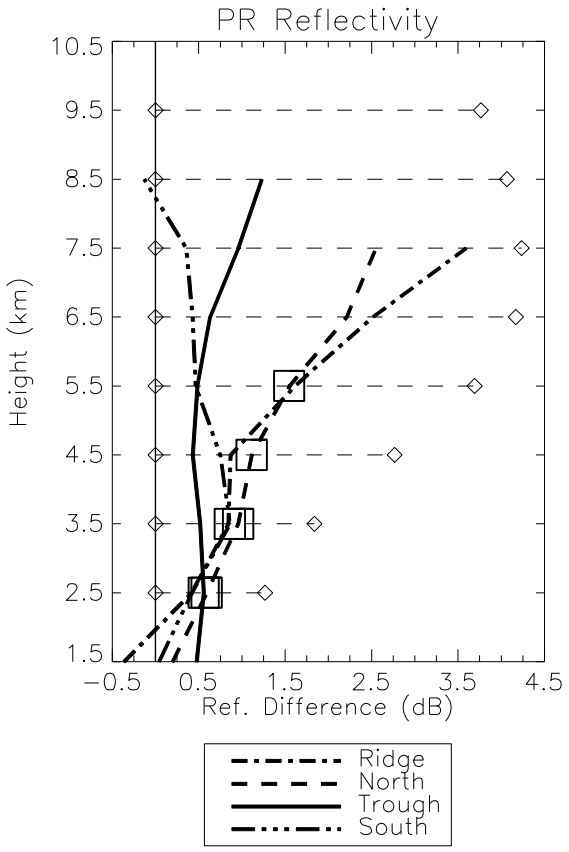

862

863 FIG. 4. Precipitation Radar (PR) convective reflectivity (only values classified as convective are
864 used) differences between East Pacific developing waves (EPDWs) and nondeveloping waves
865 (NDWs; i.e., EPDW minus NDW values) as a function of height and wave phase *valid over the*
866 *East Pacific* valid for July–August only. The dashed horizontal lines depict the value of half the
867 standard deviation at each height, and the squares indicate EPDW values that are significantly
868 greater than the corresponding NDW values valid at the 99% level.

869
870
871
872
873
874
875

List of Tables

946

947 TABLE 1. Definitions and acronyms associated with various wave categories used in this study.

Wave Category	Acronym	Definition
East Atlantic developing wave	EADW	Wave developed a tropical depression over the East Atlantic longitude band
West Atlantic – Caribbean developing wave	WACDW	Wave developed a tropical depression over the West Atlantic or Caribbean longitude band
East Pacific developing wave	EPDW	Wave developed a tropical depression over the East Pacific longitude band
Nondeveloping wave	NDW	Wave never developed a tropical cyclone of at least tropical storm strength

948

949

950

951

952

953

954

955

956

957

958

959

960

961

962

963

964

TABLE 2. The number of distinct easterly waves and data points used for the trough composites of nondeveloping waves (NDWs), East Atlantic developing waves (EADWs), West Atlantic − Caribbean developing waves (WACDWs), and East Pacific developing waves (EPDWs). The numbers of distinct waves are valid over the full analysis domain (ALL) while the trough points are valid over individual longitude bands (bands defined as in Fig. 1). The asterisk indicates wave categories that are valid for July–August only. The number of individual NDWs is an estimate and includes an estimate of uncertainty because of the difficulty in counting these waves (see text). Finally, the missing values are for those composites that were unavailable.

Sample Sizes

	Distinct AEWs	**Trough Points**				
	ALL	EPC	CAR	WAT	EAT	AFR
NDW	330±40	2582	1695	1978	1737	2505
EADW	28	–	–	–	138	313
WACDW	37	–	102	290	317	436
EPDW*	68	267	358	361	287	392
NDW*	100±15	612	449	467	454	573

TABLE 3. The fractional coverage by IR brightness temperatures ≤240 K and ≤210 K for East Atlantic developing wave (EADW), West Atlantic – Caribbean developing wave (WACDW), and nondeveloping wave (NDW) phases valid over various longitude bands. The bold (italic) numbers indicate values that are significantly greater (less) than the corresponding NDW values valid at the 99% level.

IR Brightness Temperature Thresholds

Africa

	240 K				*210 K*			
	Ridge	*Northerly*	*Trough*	*Southerly*	*Ridge*	*Northerly*	*Trough*	*Southerly*
EADW	**0.097**	**0.111**	**0.088**	**0.082**	**0.017**	**0.021**	0.015	**0.014**
WACDW	0.068	**0.085**	**0.083**	**0.079**	0.013	**0.017**	**0.015**	**0.013**
NDW	0.061	0.073	0.071	0.065	0.010	0.014	0.013	0.010

East Atlantic

	240 K				*210 K*			
	Ridge	*Northerly*	*Trough*	*Southerly*	*Ridge*	*Northerly*	*Trough*	*Southerly*
EADW	0.064	**0.094**	**0.094**	0.085	0.006	**0.009**	**0.010**	0.009
WACDW	0.046	0.064	**0.086**	*0.069*	0.004	0.004	**0.008**	0.005
NDW	0.072	0.059	0.075	0.088	0.005	0.004	0.006	0.007

West Atlantic

	240 K				*210 K*			
	Ridge	*Northerly*	*Trough*	*Southerly*	*Ridge*	*Northerly*	*Trough*	*Southerly*
WACDW	0.077	**0.067**	**0.103**	**0.110**	0.007	**0.008**	**0.011**	**0.015**
NDW	0.062	0.045	0.056	0.068	0.005	0.004	0.005	0.006

Caribbean

	240 K				*210 K*			
	Ridge	*Northerly*	*Trough*	*Southerly*	*Ridge*	*Northerly*	*Trough*	*Southerly*
WACDW	0.148	**0.162**	**0.169**	**0.163**	0.025	**0.029**	**0.032**	0.029
NDW	0.116	0.119	0.130	0.131	0.017	0.019	0.022	0.022

TABLE 4. Percentage convective coverage as a function of wave phase for East Atlantic developing waves (EADWs), West Atlantic − Caribbean developing waves (WACDWs), and nondeveloping waves (NDWs) valid over various longitude bands. The bold and italic values are as in Table 3.

	Convective Coverage (%)			
		Africa		
	Ridge	*Northerly*	*Trough*	*Southerly*
EADW	1.11	**1.16**	0.96	0.91
WACDW	0.74	0.91	0.86	0.89
NDW	0.78	0.76	0.80	0.78
		East Atlantic		
	Ridge	*Northerly*	*Trough*	*Southerly*
EADW	0.98	**1.48**	1.41	1.18
WACDW	1.18	1.07	1.24	1.10
NDW	1.02	1.07	1.16	1.11
		West Atlantic		
	Ridge	*Northerly*	*Trough*	*Southerly*
WACDW	1.44	1.42	**1.70**	1.59
NDW	1.25	1.33	1.43	1.46
		Caribbean		
	Ridge	*Northerly*	*Trough*	*Southerly*
WACDW	1.77	2.03	1.76	1.81
NDW	1.70	1.66	1.78	1.73

TABLE 5. As in Table 4, except for lightning flash rates (flashes day^{-1}).

Lightning Flash Rates

Africa

	Ridge	*Northerly*	*Trough*	*Southerly*
EADW	179.2	133.2	109.0	153.8
WACDW	139.6	128.7	115.1	127.4
NDW	110.7	103.0	107.1	109.7

East Atlantic

	Ridge	*Northerly*	*Trough*	*Southerly*
EADW	3.5	4.6	6.0	7.6
WACDW	1.0	3.3	5.0	6.1
NDW	2.4	3.0	4.4	8.5

West Atlantic

	Ridge	*Northerly*	*Trough*	*Southerly*
WACDW	10.8	26.8	23.6	17.8
NDW	23.1	24.6	17.0	14.5

Caribbean

	Ridge	*Northerly*	*Trough*	*Southerly*
WACDW	96.8	135.6	115.7	130.4
NDW	83.9	94.6	104.6	107.2

TABLE 6. Mean polarization corrected temperatures at 37.0 and 85.5 GHz using 37.0-GHz values ≤260 K and 85.5-GHz values ≤200 K (i.e., values associated with deep convection) for East Atlantic developing wave (EADW), West Atlantic – Caribbean developing wave (WACDW), and nondeveloping wave (NDW) phases valid over various longitude bands. No EADW or WACDW values are significantly different from those of NDWs valid at the 99% level.

Polarization Corrected Temperatures

Africa

	37.0				*85.5*			
	Ridge	*Northerly*	*Trough*	*Southerly*	*Ridge*	*Northerly*	*Trough*	*Southerly*
EADW	250.3	251.0	251.2	251.9	174.9	175.8	177.0	177.1
WACDW	251.5	252.2	251.6	251.6	175.1	176.0	176.3	176.1
NDW	251.4	251.7	251.7	251.7	176.4	176.4	177.0	177.7

East Atlantic

	37.0				*85.5*			
	Ridge	*Northerly*	*Trough*	*Southerly*	*Ridge*	*Northerly*	*Trough*	*Southerly*
EADW	257.4	256.4	256.5	256.1	185.9	184.0	184.3	183.0
WACDW	254.4	256.8	256.6	256.4	185.9	184.3	185.0	185.3
NDW	257.0	257.0	256.7	256.2	186.3	185.3	185.6	185.3

West Atlantic

	37.0				*85.5*			
	Ridge	*Northerly*	*Trough*	*Southerly*	*Ridge*	*Northerly*	*Trough*	*Southerly*
WACDW	255.8	254.5	255.2	255.5	183.7	181.5	183.5	182.2
NDW	255.3	254.7	255.3	255.6	183.0	182.0	183.1	183.4

Caribbean

	37.0				*85.5*			
	Ridge	*Northerly*	*Trough*	*Southerly*	*Ridge*	*Northerly*	*Trough*	*Southerly*
WACDW	255.5	252.6	253.2	253.3	181.0	177.5	177.4	178.4
NDW	253.7	253.5	253.3	253.2	178.0	178.6	178.6	178.5

TABLE 7. The fractional coverage by IR brightness temperatures ≤240 K and ≤210 K, mean polarization corrected temperatures (K) at 37.0 and 85.5 GHz using the same thresholds as in Table 6, convective coverage (%), and lightning flash rates (flashes day^{-1}) for developing and nondeveloping waves (30−50% Dev. and 30−50% ND, respectively) that were assigned a 30−50% probability of development within the next 48 hours by the National Hurricane Center. Note that none of the 30–50% Dev. values are significantly different from the corresponding 30–50% ND values valid at the 99% level.

IR Brightness Temperature Thresholds

		Ridge	*Northerly*	*Trough*	*Southerly*
30-50% Dev.	240 K	0.108	0.115	0.154	0.172
	210 K	0.011	0.014	0.021	0.024
30-50% ND	240 K	0.104	0.079	0.133	0.125
	210 K	0.015	0.009	0.021	0.021

Polarization Corrected Temperatures

		Ridge	*Northerly*	*Trough*	*Southerly*
30-50% Dev.	37.0	254.7	254.7	255.0	255.4
	85.5	185.4	182.1	182.2	183.0
30-50% ND	37.0	255.7	256.7	256.1	255.0
	85.5	180.1	183.1	183.6	180.6

Convective Coverage

	Ridge	*Northerly*	*Trough*	*Southerly*
30-50% Dev.	1.56	1.48	1.93	1.93
30-50% ND	1.62	1.20	1.38	1.69

LIS Flash Rates

	Ridge	*Northerly*	*Trough*	*Southerly*
30-50% Dev.	93.2	40.4	58.0	43.5
30-50% ND	38.3	8.2	10.5	89.1

TABLE 8. The factional coverage by IR brightness temperatures ≤240 K and ≤210 K for East Pacific developing wave (EPDW) and nondeveloping wave (NDW) phases valid over various longitude bands using only data valid for July and August. The bold and italic values are as in Table 3.

IR Brightness Temperature Thresholds (July-August Only)

Africa

	240 K				*210 K*			
	Ridge	*Northerly*	*Trough*	*Southerly*	*Ridge*	*Northerly*	*Trough*	*Southerly*
EPDW	0.083	*0.100*	*0.093*	*0.068*	0.014	*0.017*	*0.016*	0.011
NDW	0.089	0.116	0.105	0.081	0.017	0.023	0.019	0.013

East Atlantic

	240 K				*210 K*			
	Ridge	*Northerly*	*Trough*	*Southerly*	*Ridge*	*Northerly*	*Trough*	*Southerly*
EPDW	0.054	0.048	0.057	0.049	0.004	0.003	0.004	0.002
NDW	0.048	0.052	0.064	0.053	0.003	0.003	0.005	0.004

West Atlantic

	240 K				*210 K*			
	Ridge	*Northerly*	*Trough*	*Southerly*	*Ridge*	*Northerly*	*Trough*	*Southerly*
EPDW	0.051	0.041	0.054	0.058	0.004	0.003	0.004	0.005
NDW	0.037	0.042	0.047	0.050	0.003	0.003	0.004	0.004

Caribbean

	240 K				*210 K*			
	Ridge	*Northerly*	*Trough*	*Southerly*	*Ridge*	*Northerly*	*Trough*	*Southerly*
EPDW	0.141	0.151	0.156	**0.166**	0.022	0.026	0.027	**0.029**
NDW	0.124	0.146	0.149	0.136	0.020	0.026	0.027	0.023

East Pacific

	240 K				*210 K*			
	Ridge	*Northerly*	*Trough*	*Southerly*	*Ridge*	*Northerly*	*Trough*	*Southerly*
EPDW	**0.099**	**0.130**	**0.154**	**0.180**	0.010	**0.016**	**0.022**	**0.024**
NDW	0.073	0.084	0.116	0.122	0.006	0.008	0.013	0.014

TABLE 9. Lightning flash rates (flashes day^{-1}) for East Pacific developing wave (EPDW) and nondeveloping wave (NDW) phases valid over various longitude bands using only data valid for July and August. The bold and italic values are as in Table 3.

Lightning Flash Rates (July-August Only)

		Africa		
	Ridge	*Northerly*	*Trough*	*Southerly*
EPDW	123.6	131.6	138.4	109.6
NDW	206.7	143.8	142.4	120.8
		East Atlantic		
	Ridge	*Northerly*	*Trough*	*Southerly*
EPDW	2.8	1.4	3.1	3.7
NDW	1.2	0.6	3.0	3.5
		West Atlantic		
	Ridge	*Northerly*	*Trough*	*Southerly*
EPDW	12.1	14.2	19.8	16.2
NDW	8.2	16.6	14.8	17.4
		Caribbean		
	Ridge	*Northerly*	*Trough*	*Southerly*
EPDW	104.8	138.3	137.4	115.5
NDW	112.0	161.1	126.1	119.6
		East Pacific		
	Ridge	*Northerly*	*Trough*	*Southerly*
EPDW	58.5	**68.2**	**72.8**	**69.5**
NDW	18.9	32.2	37.0	36.4

TABLE 10. A summary of the convective parameters that provide the greatest distinction between nondeveloping waves and East Atlantic developing waves (EADWs), West Atlantic – Caribbean developing waves (WACDWs), and East Pacific developing waves (EPDWs) over various regions (EAT = East Atlantic, WAT = West Atlantic, CAR = Caribbean, and EPC = East Pacific) in various phases. Suggested thresholds to initially be tested to determine the utility of these parameters for tropical cyclogenesis forecasting are also provided. Note that the 240 K and 210 K IR coverage thresholds are nondimensional, while the flash rate threshold has units of flashes day^{-1}.

Convective Parameters and Thresholds

Wave Type	*Location*	*Phase*	*Parameter*	*Threshold*
EADW	EAT	northerly/ trough	240 K IR coverage	0.090
EADW	EAT	northerly/ trough	210 K IR coverage	0.009
WACDW	WAT	southerly	240 K IR coverage	0.085
WACDW	WAT	southerly	210 K IR coverage	0.009
WACDW	CAR	trough	240 K IR coverage	0.155
WACDW	CAR	trough	210 K IR coverage	0.029
EPDW	CAR	southerly	240 K IR coverage	0.150
EPDW	EPC	trough/ southerly	240 K IR coverage	0.140
EPDW	EPC	northerly/ trough/ southerly	Flash rate	60.0